Overview of Nuclear Deformation in Low-Energy Experiments

Kathrin Wimmer

GSI Helmholtzzentrum für Schwerionenforschung

24. February 2023

European Research Council

Established by the European Commission

Outline

1. Experimental determination of nuclear deformation
2. Deformation in the $A = 90 - 100$ mass region
3. The case of ^{96}Ru and ^{96}Zr
4. Summary

Experimental determination of nuclear deformation

Observations of deformation

observations:

- electric quadrupole moments and quadrupole transition rates are orders of magnitude larger than single-particle estimates (quantum transition of a single proton)
  $\rightarrow$ interpretation as collective excitations
- already deuteron has non-zero quadrupole moment $\rightarrow$ nuclear force non-spherical
- sequence of low-energy states $J(J+1)$
  $\rightarrow$ quantum mechanical rotations
  $\rightarrow$ breaking of spherical symmetry and deformation
- many physical observables can be interpreted as signs of deformation
- usually some degree of model dependence is involved in the analysis
- all nuclei are somewhat deformed, for ^{208}Pb $\beta_2 = 0.055$

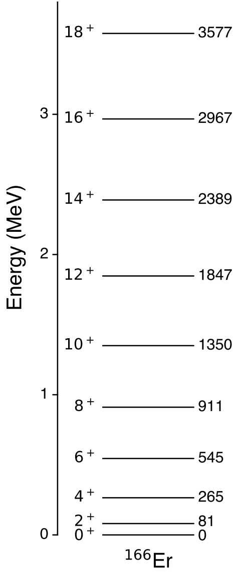

Rotational model

$$R(\theta,\phi) = R_0 \left(\sum_{\lambda=0}^{\infty} \sum_{\mu=-\lambda}^{\lambda} \alpha_{\lambda\mu} Y_{\lambda\mu}(\theta,\phi) \right)$$

- incompresibility of nuclear matter $\rightarrow$ volume conservation
- dipole term ($\lambda = 1$) just a shift of center of mass $\rightarrow$ quadrupole term ($\lambda = 2$) first important one

Rotational model

$$R(\theta,\phi) = R_0\left(\sum_{\lambda=0}^{\infty}\sum_{\mu=-\lambda}^{\lambda}\alpha_{\lambda\mu}Y_{\lambda\mu}(\theta,\phi)\right)$$

- incompresibility of nuclear matter $\rightarrow$ volume conservation
- dipole term ($\lambda = 1$) just a shift of center of mass $\rightarrow$ quadrupole term ($\lambda = 2$) first important one

- triaxial degrees of freedom:

$$\begin{aligned} \alpha_{02} &= \beta\cos\gamma \\ \alpha_{22} = \alpha_{2-2} &= \frac{1}{\sqrt{2}}\beta\sin\gamma \end{aligned}$$

- β is the axial elongation, γ asymmetry from an axial shape

$$\beta = \frac{4}{3}\sqrt{\frac{\pi}{5}}\left(\frac{c-a}{R}\right)$$

- oblate $\beta < 0$, prolate $\beta > 0$

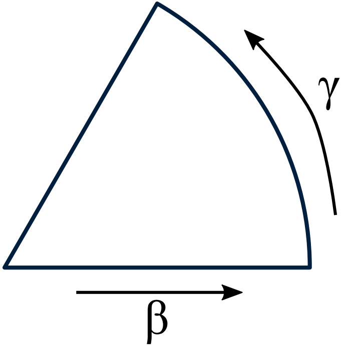

Rotational model

$$R(\theta,\phi) = R_0\left(\sum_{\lambda=0}^{\infty}\sum_{\mu=-\lambda}^{\lambda}\alpha_{\lambda\mu}Y_{\lambda\mu}(\theta,\phi)\right)$$

- incompresibility of nuclear matter $\rightarrow$ volume conservation
- dipole term ($\lambda = 1$) just a shift of center of mass $\rightarrow$ quadrupole term ($\lambda = 2$) first important one

- triaxial degrees of freedom:

$$\begin{aligned}\alpha_{02} &= \beta\cos\gamma \\ \alpha_{22} = \alpha_{2-2} &= \frac{1}{\sqrt{2}}\beta\sin\gamma\end{aligned}$$

- β is the axial elongation, γ asymmetry from an axial shape

$$\beta = \frac{4}{3}\sqrt{\frac{\pi}{5}}\left(\frac{c-a}{R}\right)$$

- oblate $\beta < 0$, prolate $\beta > 0$

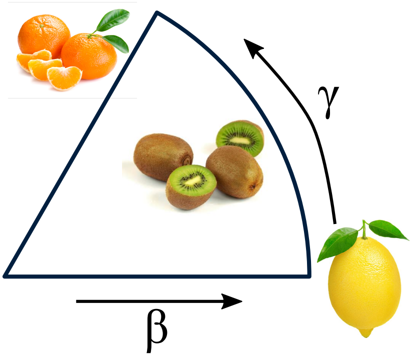

Rotational model

- measuring β or γ is not possible
- need to use nuclear models to estimate the deformation from the data
- rotational model:

$$E(J) = \frac{\hbar^2}{2I}\left(J(J+1) + K(K+1)\right)$$

- with moment of inertia for an ellipsoid (rigid, first order)

$$I_{\mathrm{rigid}} = \frac{2}{5} AMR_0^2 \left(1 + 0.31\beta\right)$$

- increasing deformation β
  $\rightarrow$ smaller energy spacing
- assumption: constant I along band
- superposition of vibrational excitations below the pairing gap

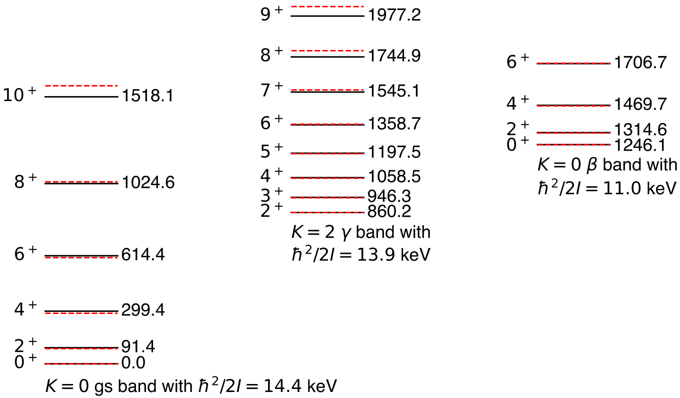

Rotational model

- experimental moments of inertia are intermediate between a rigid body and irrotational flow
  $\rightarrow$ nuclear superfluidity due to the pairing force

- rigid body with deformation β

$$I_{\text{rigid}} = \frac{2}{5} A M R_0^2 (1 + 0.31\beta)$$

- irrotational flow

$$I_{\text{irr}} = \frac{9}{8\pi} M R_0^2 \beta^2$$

- experimental data approximated by

$$I_{\text{exp}} = \frac{\hbar^2 \beta^2 A^{7/3}}{400[\text{MeV}]}$$

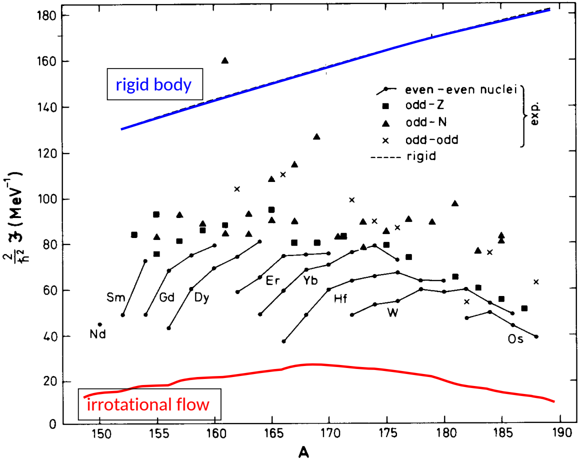

$\mathfrak{J}_R$ > $\mathfrak{J}_{\text{exp}}$ > $\mathfrak{J}_F$

Rotational model

- spectroscopy of first few excited states
- low $E(2^+_1)$ indicates collective nature
- energy ratio $R_{4/2} = \frac{E(4^+_1)}{E(2^+_1)}$, for vibrational $R_{4/2} = 2$, for rotational $R_{4/2} = 3.333$

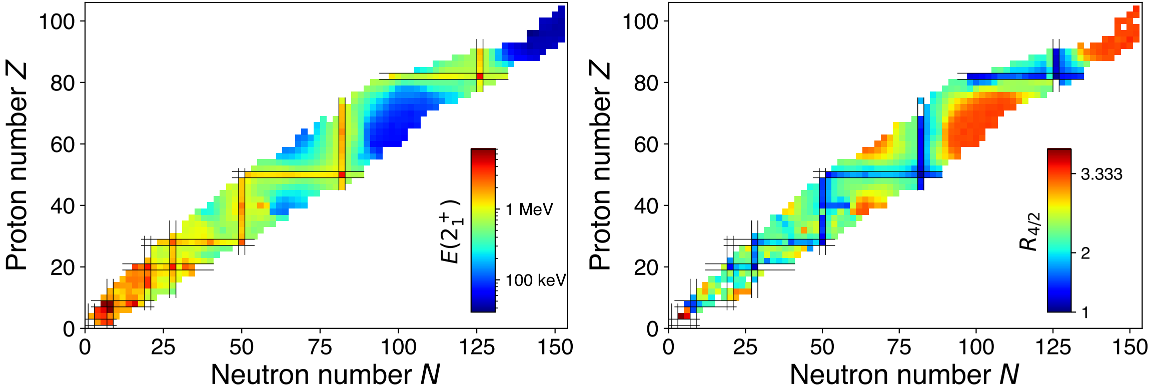

Charge radii

- detailed spectroscopy of the atomic spectrum allows to draw conclusions on the nuclear size
- mean square radius of a deformed nucleus:

$$\langle r^2 \rangle = \underbrace{\frac{3}{5}\left(R_0 A^{1/3}\right)^2}_{\text{spherical, liquid drop}} + \underbrace{\frac{3}{4\pi}\left(R_0 A^{1/3}\right)^2 \beta^2}_{\text{deformation}}$$

- smooth increase with mass

$$\frac{\delta \langle r^2 \rangle_{\text{sph}}}{\delta A} = \frac{2}{5} R_0^2 A^{-1/3} \sim 0.1\ \text{fm}^2 \text{ for } A \sim 200$$

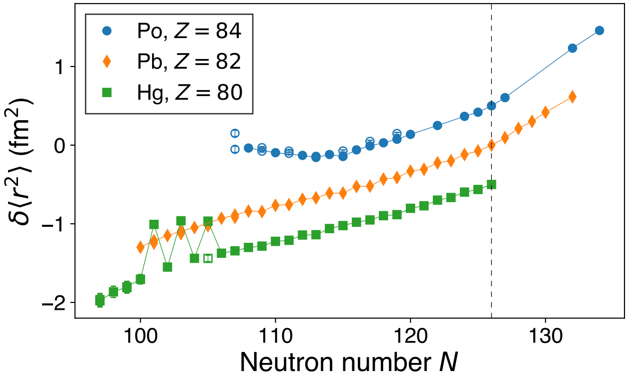

- β is the charge deformation
- experimentally determined from isotope shifts (difference in optical transition frequency of two isotopes)
- for stable isotopes with electron scattering
- matter radii from interaction cross section measurements

Quadrupole moments

- electric quadrupole moment

$$eQ_0 = \int \left(3z^2 - r^2\right)\rho(r,\theta,\phi)\mathrm{d}^3 r = \sqrt{\frac{16\pi}{5}}\int r^2 Y_{20}(\theta,\phi)\rho(r,\theta,\phi)\mathrm{d}^3 r$$

- intrinsic quadrupole moment

$$Q_0 = ZR_0^2 \frac{3}{\sqrt{5\pi}}\left(\beta_2 + \frac{2}{7}\sqrt{\frac{5}{\pi}}\beta_2^2 + \cdots\right)$$

- spectroscopic quadrupole moment (observed in the lab)

$$Q_s = \frac{3K^2 - I(I+1)}{(I+1)(2I+3)}Q_0, \qquad \text{implies } Q_s = 0, \text{ for } I = 0 \text{ or } 1/2$$

- hyperfine splitting depends on magnetic dipole and electric quadrupole coupling of electrons to the nuclear moments

$$E(F) = \frac{1}{2}AC + B\frac{3/4C(C+1) - I(I+1)J(J+1)}{2I(2I-1)J(2J-1)}, \text{ with } C = F(F+1) - I(I+1) - J(J+1)$$

I nuclear angular momentum, J electron angular momentum, F total angular momentum
$A = \mu_I B_e(0)/(IJ)$ and $B = eQ_s V_{zz}(0)$
$B_e(0)$ magnetic field and $V_{zz}(0)$ electric field gradient of the electron at the nucleus

Quadrupole moments

Failure of the nuclear shell model to give correct quadrupole moments is in contrast to the situation with nuclear magnetic moments, which can all be accounted for by a suitable admixture of states of a single nucleon. In the shell model approximation, these large quadrupole moments must represent a considerable contribution from the protons in the closed shells. The polarization of this core would presumably require a sharing of angular momentum between the protons of the incomplete shell and those of the closed shells. The magnitude of the polarization, however, and the resulting large asymmetry of the nucleon distribution is hardly consistent with the single particle-central field quantization which is the basis of the shell structure model.

C. H. Townes, H. M. Foley, and W. Low, Phys. Rev. **76** (1949) 1415.

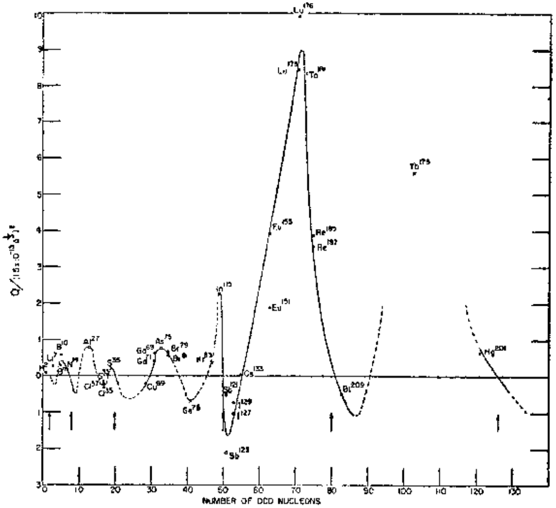

Transition strength

- reduced transition probability

$$B(\Pi\lambda) = \frac{|\langle I_f || \Pi\lambda || I_i \rangle|}{2I_i + 1}$$

- large $B(E2)$ values indicate similar structure of states
- is related to the intrinsic quadrupole moment

$$eQ_0 = \sqrt{\frac{16\pi}{5}} \frac{\langle I_f || E2 || I_i \rangle}{\sqrt{2I_i + 1} \langle I_i K 20 | I_f 0 \rangle}$$

$$B(E2;\ I_i \to I_f) = \frac{5}{16\pi} (eQ_0)^2 \langle I_i K 20 | I_f 0 \rangle^2$$

- in rotational model

$$B(E2;\ 0_1^+ \to 2_1^+) = \left(\frac{3}{4\pi} ZeR^2 \beta_2 \right)^2$$

- reduced transition probability and lifetime are related:

$$B(E2) = \frac{8.177 \cdot 10^{-10}}{\tau E_\gamma^5} \frac{1}{1 + \alpha}$$

E in keV, τ (partial) lifetime in s, $B(E2)$ in $e^2\mathrm{fm}^4$, α conversion coefficient

Transition strength

- $B(E2)$ can be obtained from lifetimes of excited states

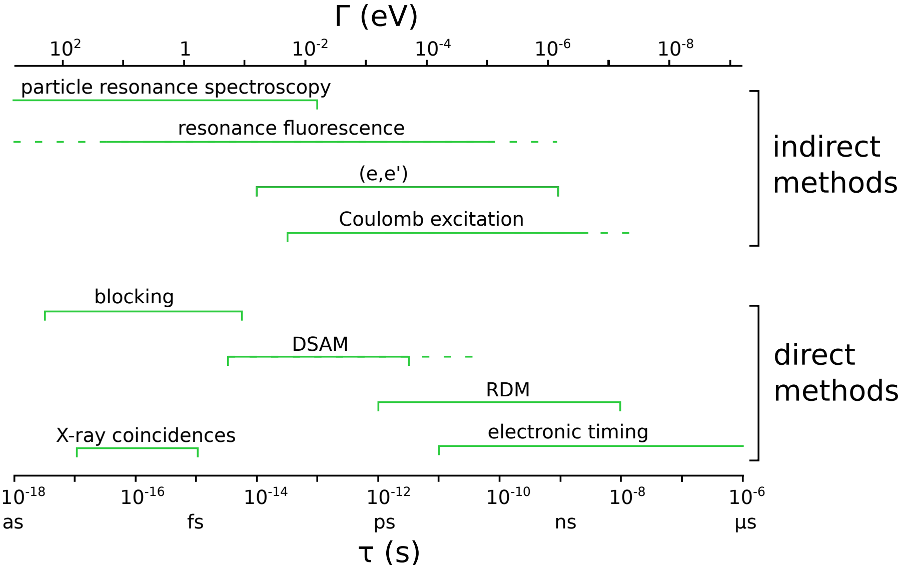

Transition strengths over the nuclear chart

- extraction of the $B(E2)$ values of require some modeling
- energies are a good indicator of nuclear structure

$$B(E2;\, 0_1^+ \to 2_1^+) = (124 \pm 41)\, \frac{Z^2}{E(2_1^+)A}$$

L. Grodzins, Phys. Lett. **2** (1962) 88.

- energies not sensitive to the details of the wave function

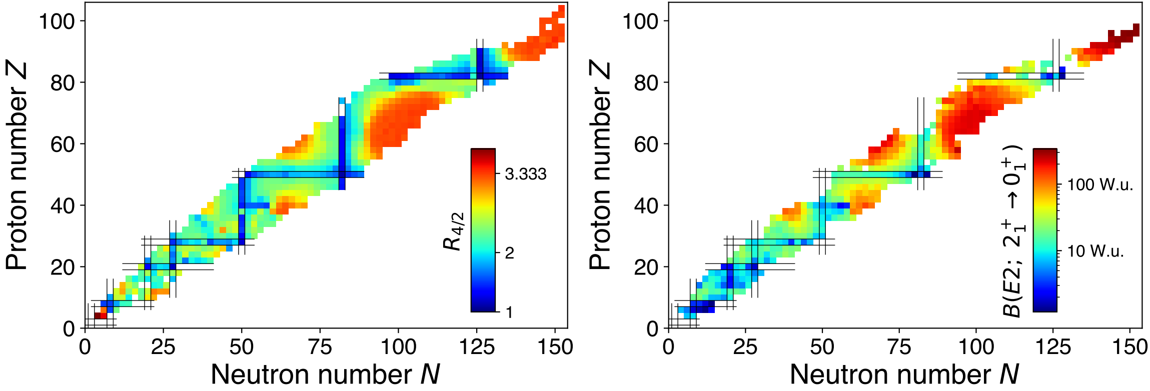

Transition strengths over the nuclear chart

- Weisskopf units, single-particle estimate, how many nucleons participate in the excitation
- assuming axial symmetry, deformation can be extracted from $B(E2)$ values

$$\beta_2 = \frac{4\pi}{3eZR^2}\sqrt{B(E2;\, 0_1^+ \rightarrow 2_1^+)}$$

- spherical magic nuclei
- $\beta = 0.3$ for well-deformed rare-earth (green) and super-heavy nuclei (red)
- outliers with very large β $\rightarrow$ limitations of the approximations made

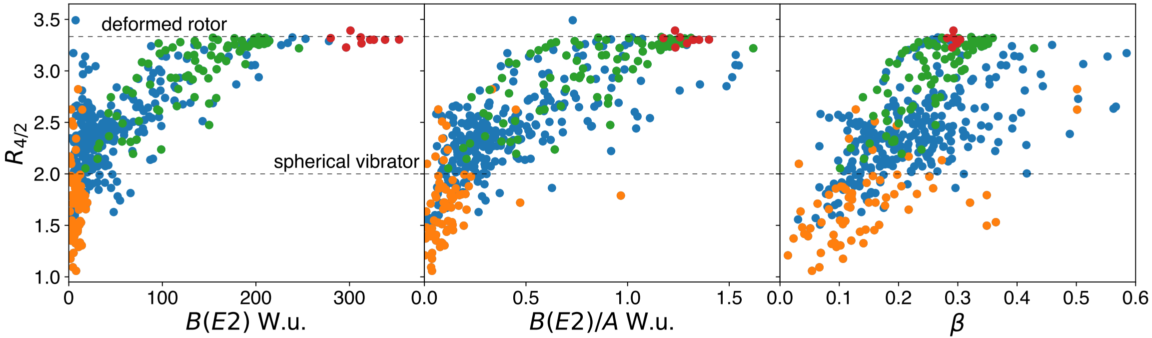

Coulomb excitation

- probe of collective shape degrees of freedom
- excitation of the nucleus in the electromagnetic field of the target $V(t)$

$$\left(\frac{\mathrm{d}\sigma}{\mathrm{d}\Omega}\right)_{i\to f} = \left(\frac{\mathrm{d}\sigma}{\mathrm{d}\Omega}\right)_{\mathrm{Ruth}} |a_{i\to f}|^2$$

- perturbation theory

$$a_{i\to f} = \frac{1}{i\hbar}\int_{-\infty}^{\infty} \mathrm{d}t\, e^{i\omega t}\, \langle f|V(t)|i\rangle$$

- multipole expansion

$$\sigma(\pi\lambda)_{i\to f} \propto B(\pi\lambda;\, I_i \to I_f)$$

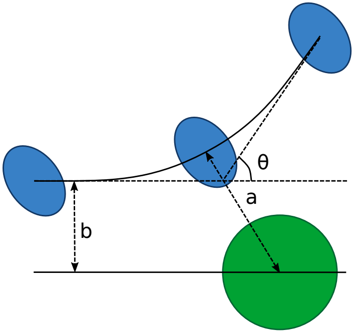

θ scattering angle
b impact parameter
a distance of closest approach

- employ high Z probe, typically Sn or Pb
- other processes contribute to the excitation
- for pure Coulomb excitation, the contribution from nuclear processes has to be eliminated

Coulomb excitation

- at high beam energies, above Coulomb barrier, main uncertainties come from nuclear excitations and reaction modeling, few percent for $B(E2)$
- excitation is limited to 2^+ states which can feed the state of interest

$$\sigma(\pi\lambda)_{i\to f} \propto B(\pi\lambda;\ I_i \to I_f)$$

- at Coulomb barrier energies, longer interaction times allow for multi-step processes $\rightarrow$ excitation of 4^+, 2^+_2, 0^+_2, etc states
- in addition the cross section becomes sensitive to the static quadrupole moment through the re-orientation effect

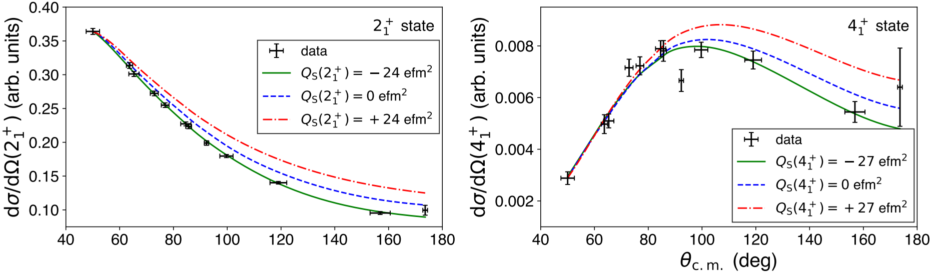

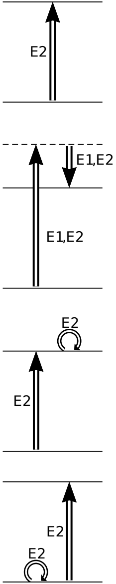

Coulomb excitation

- full two-dimensional χ^2 surface for $\langle 2_1^+ || E2 || 0_1^+ \rangle$ and $\langle 2_1^+ || E2 || 2_1^+ \rangle$ shows the correlation of the two values
- combination with other observable, here τ from direct lifetime measurement, allows for determination of sign and magnitude of the matrix elements

M. Zielinska et al., Eur. Phys. J. A **52** (2016) 99.

- remember: quadrupole moments from hyperfine studies are only for $J > 1/2$ and ground or long-lived states
- only way to access the quadrupole moments of excited states
- sensitivity depends on the complexity of the level scheme and statistics
- Coulomb excitation also provides access to $E3$ moments

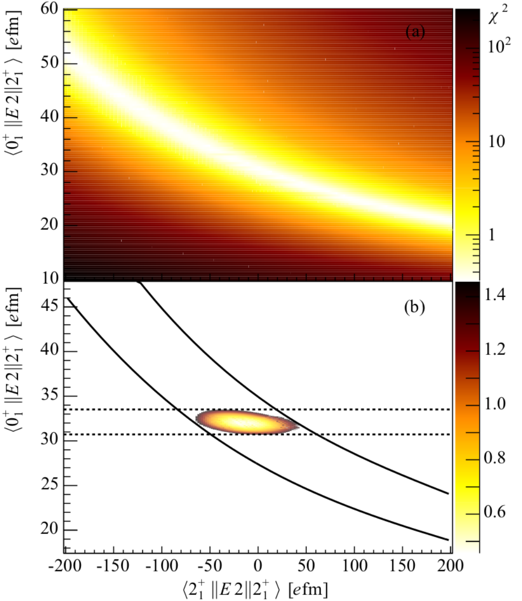

Quadrupole invariants

quadrupole rotationally invariant sum rules provide a more model independent measure of the shape

K. Kumar, Phys. Rev. Lett. **28** (1972) 249, D. Cline, Annu. Rev. Nucl. Part. Sci. **36** (1986) 681.

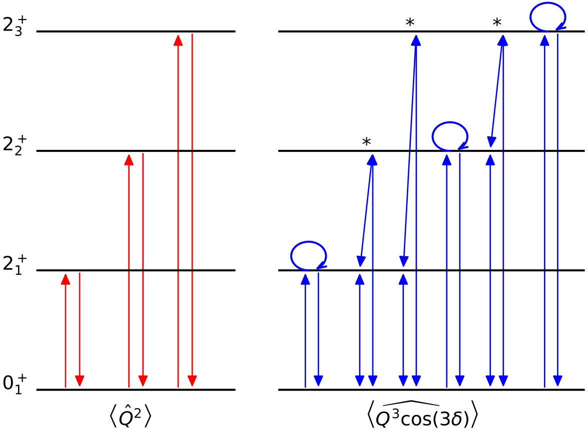

J. Henderson, Phys. Rev. C **102** (2020) 054306.

- charge distribution $E(\lambda,\mu)$ in the intrinsic frame:

$$E(2,0) = Q\cos(\delta), E(2,\pm1) = 0, E(2,\pm2) = \frac{1}{\sqrt{2}}Q\sin(\delta)$$

- invariants

$$\langle Q^2 \rangle = \sqrt{\frac{5}{2I_s+1}} \sum_i \langle s||E2||i\rangle\langle i||E2||s\rangle \begin{Bmatrix} 2 & 2 & 0 \\ I_s & I_s & I_i \end{Bmatrix}$$

$$\langle Q^3 cos(3\delta)\rangle = -\sqrt{\frac{35}{2}}\frac{1}{2I_s+1} \times$$

$$\sum_{i,j} \langle s||E2||i\rangle\langle i||E2||j\rangle\langle j||E2||s\rangle \begin{Bmatrix} 2 & 2 & 2 \\ I_s & I_j & I_i \end{Bmatrix}$$

- relates to deformation parameter

$$\langle Q^2 \rangle = \left(\frac{3}{4\pi}ZR_0^3\right)^2 \langle \beta^2 \rangle, \qquad \delta = \gamma$$

Quadrupole invariants

- higher order products give also access to the fluctuations of Q and δ

$$\sigma(Q^2) = \sqrt{\langle Q^4 \rangle - \langle Q^2 \rangle^2} \qquad \text{and} \qquad \sigma(\cos(3\delta)) = \sqrt{\frac{\langle Q^6 \cos^2(3\delta)\rangle}{\langle Q^6 \rangle} - \left(\frac{\langle Q \cos(3\delta)\rangle}{\langle Q^2 \rangle^{3/2}}\right)^2}$$

- experimentally challenging as many matrix elements, with sign, have to be measured

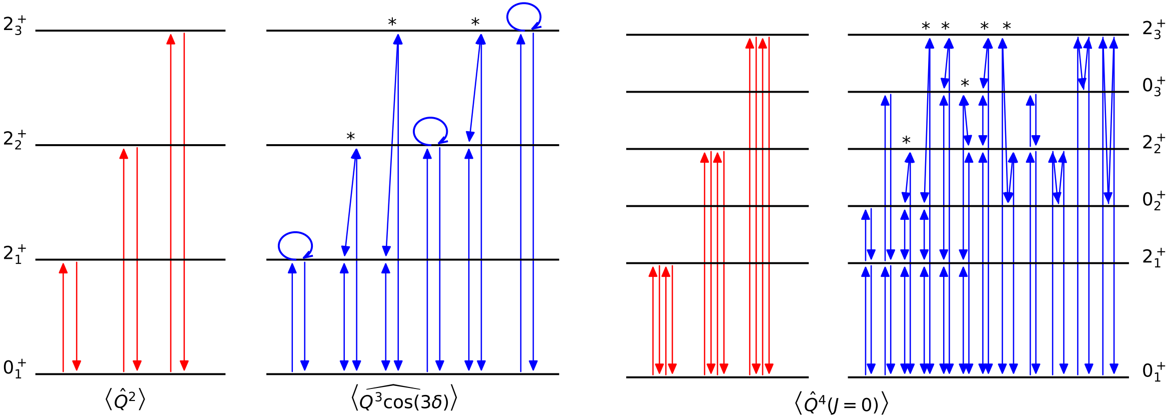

Triaxial degrees of freedom

- axial γ-rigid rotor of the Davydov-Filippov model, stable minimum
- low-lying γ band, strong decay to 2_1^+

A. Davydov, G. Filippov, Nucl. Phys. **8** (1958) 237.

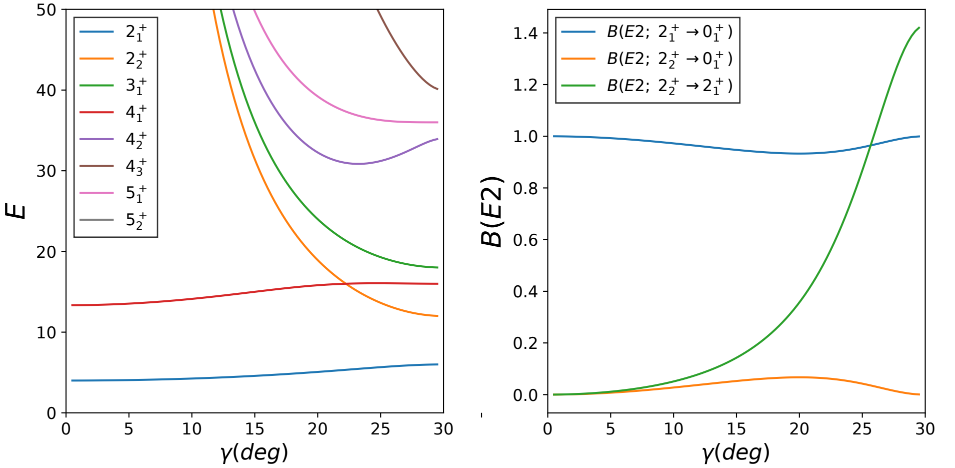

Triaxial degrees of freedom

- γ-soft, γ independent potential

L. Wilets, M. Jean, Phys. Rev. **102** (1956) 788.

- excitation energies not very sensitive to differences of the model

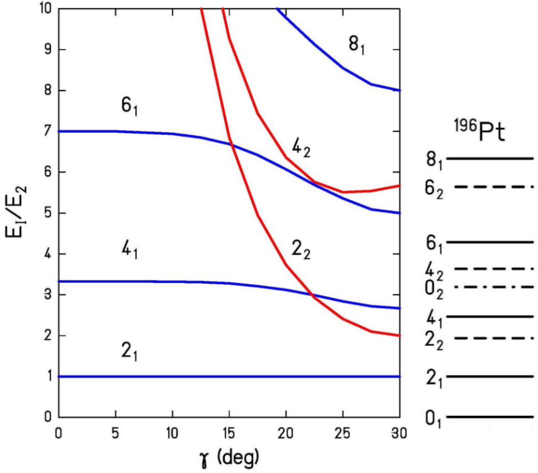

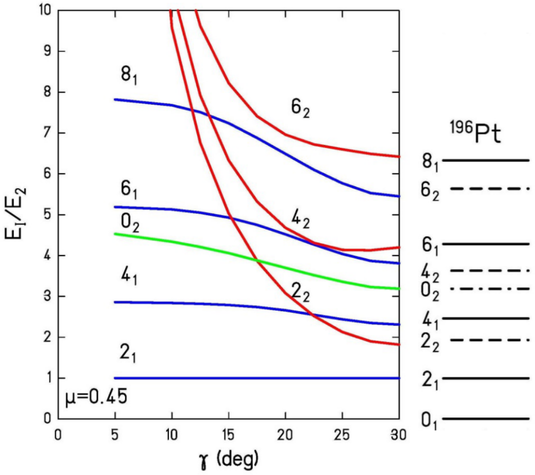

Triaxial degrees of freedom

one example: ^{76}Ge ($0\nu\beta\beta$ candidate)

- $R_{4/2} = E(4_1^+)/E(2_1^+) = 2.51$ experimentally
- γ-soft model predicts $R_{4/2} = 2.50$,
- rigid triaxial $R_{4/2} = 2.67$ for $\gamma = 30^\circ$
- $B(E2;\, 2_2^+ \to 0_1^+)/B(E2;\, 2_2^+ \to 2_1^+) = 0$ in both models
- experiment $B(E2;\, 2_2^+ \to 0_1^+)/B(E2;\, 2_2^+ \to 2_1^+) = 0.027(3)$
- analyze staggering parameter:

$$S(I) = \frac{[E(I) - E(I-1)] - [E(I-1) - E(I-2)]}{E(2_1^+)}$$

- different phase of staggering in the γ band
- consistent with predictions for a rigid-triaxial shape, but much less pronounced

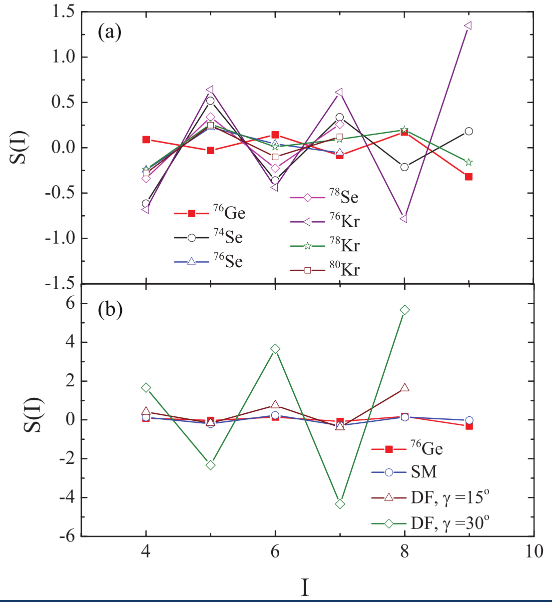

Y. Toh et al., Phys. Rev. C **87** (2013) 041304(R).

Triaxial degrees of freedom

- $\rightarrow$ analysis of quadrupole invariants
- requires knowledge of many matrix elements with their signs

A. D. Ayangeakaa et al., Phys. Rev. Lett. **123** (2019) 102501.

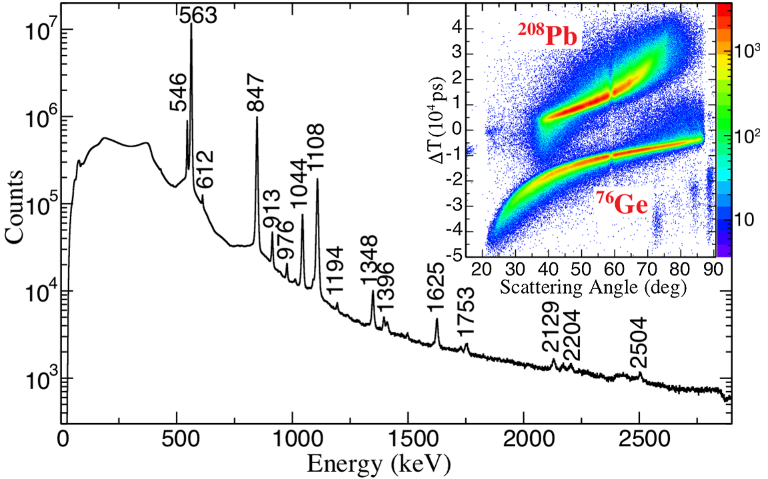

TABLE I. $E2$ matrix elements for ^{76}Ge obtained from the present analysis and comparisons with previous measurements. Note that not all matrix elements corresponding to the levels shown in Fig. 2 are given here. The complete set will be provided in a forthcoming publication [41].

	$\langle I_i \| \mathcal{M}(E2) \| I_f \rangle$ (eb)		
$I_i^\pi \rightarrow I_f^\pi$	This work	Ref. [29]	Refs. [39,40]
$0_1^+ \rightarrow 2_1^+$	0.526(2)	0.522(4)	0.550(3)
$0_1^+ \rightarrow 2_2^+$	0.089(3)	0.069(10)	$\|0.081(14)\|$
$0_1^+ \rightarrow 2_3^+$	0.061(3)		
$0_1^+ \rightarrow 2_4^+$	0.054(4)		
$0_1^+ \rightarrow 2_5^+$	0.023(6)		
$2_1^+ \rightarrow 2_1^+$	−0.24(2)	−0.14(4)	−0.19(6)
$2_1^+ \rightarrow 2_2^+$	$0.535^{+0.003}_{-0.007}$	0.54(3)	$\|0.71(7)\|$
$2_1^+ \rightarrow 2_3^+$	$-0.126^{+0.006}_{-0.004}$		
$2_1^+ \rightarrow 2_4^+$	$0.022^{+0.008}_{-0.005}$		
$2_1^+ \rightarrow 2_5^+$	$-0.048^{+0.002}_{-0.007}$		
$2_1^+ \rightarrow 3_1^+$	0.082(5)		
$2_1^+ \rightarrow 4_1^+$	0.795(5)	0.71(4)	0.77(4)
$2_1^+ \rightarrow 4_2^+$	$-0.22^{+0.05}_{-0.03}$	0.10(2)	
$2_2^+ \rightarrow 2_2^+$	$0.26^{+0.02}_{-0.05}$	0.28(6)	
$2_2^+ \rightarrow 3_1^+$	$0.52^{+0.02}_{-0.04}$		
$2_2^+ \rightarrow 4_2^+$	0.472(6)	0.56(2)	
$4_1^+ \rightarrow 4_1^+$	$-0.26^{+0.01}_{-0.07}$	−0.01(5)	
$4_1^+ \rightarrow 6_1^+$	$1.11^{+0.03}_{-0.02}$	0.87(2)	
$6_1^+ \rightarrow 8_1^+$	$1.25^{+0.07}_{-0.10}$		
$6_1^+ \rightarrow 6_1^+$	$-0.23^{+0.09}_{-0.04}$		
$3_1^+ \rightarrow 5_1^+$	$0.9^{+0.4}_{-0.6}$		
$4_2^+ \rightarrow 3_1^+$	$0.64^{+0.03}_{-0.07}$		
$4_2^+ \rightarrow 5_1^+$	$0.9^{+0.7}_{-0.2}$		
$4_2^+ \rightarrow 6_2^+$	0.49(3)		
$6_2^+ \rightarrow 5_1^+$	$-0.74^{+0.10}_{-0.08}$		
$3_1^+ \rightarrow 3_1^+$	$0.13^{+0.08}_{-0.10}$		
$4_2^+ \rightarrow 4_2^+$	$-0.24^{+0.08}_{-0.04}$		
$4_1^+ \rightarrow 2_2^+$	0.09(2)	−0.11(1)	
$4_1^+ \rightarrow 3_1^+$	$-0.44^{+0.08}_{-0.05}$		
$4_1^+ \rightarrow 4_2^+$	0.61(1)	−0.10(3)	
$4_1^+ \rightarrow 5_1^+$	$-0.08^{+0.09}_{-0.05}$		
$4_1^+ \rightarrow 6_2^+$	$-0.186^{+0.030}_{-0.005}$		
$6_1^+ \rightarrow 4_2^+$	$0.35^{+0.05}_{-0.03}$	0.21(4)	

Triaxial degrees of freedom

- → analysis of quadrupole invariants
- requires knowledge of many matrix elements with their signs

A. D. Ayangeakaa et al., Phys. Rev. Lett. **123** (2019) 102501.

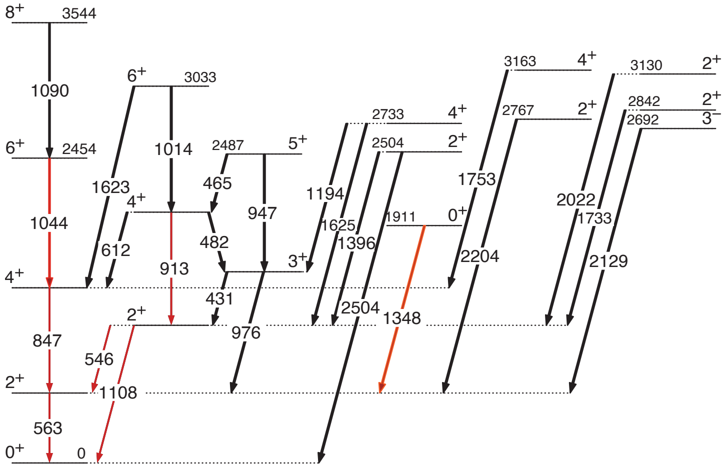

TABLE I. $E2$ matrix elements for ^{76}Ge obtained from the present analysis and comparisons with previous measurements. Note that not all matrix elements corresponding to the levels shown in Fig. 2 are given here. The complete set will be provided in a forthcoming publication [41].

	$\langle I_i \Vert \mathcal{M}(E2) \Vert I_f \rangle$ (eb)		
$I_i^\pi \to I_f^\pi$	This work	Ref. [29]	Refs. [39,40]
$0_1^+ \to 2_1^+$	0.526(2)	0.522(4)	0.550(3)
$0_1^+ \to 2_2^+$	0.089(3)	0.069(10)	|0.081(14)|
$0_1^+ \to 2_3^+$	0.061(3)		
$0_1^+ \to 2_4^+$	0.054(4)		
$0_1^+ \to 2_5^+$	0.023(6)		
$2_1^+ \to 2_1^+$	−0.24(2)	−0.14(4)	−0.19(6)
$2_1^+ \to 2_2^+$	$0.535^{+0.003}_{-0.007}$	0.54(3)	|0.71(7)|
$2_1^+ \to 2_3^+$	$-0.126^{+0.006}_{-0.004}$		
$2_1^+ \to 2_4^+$	$0.022^{+0.008}_{-0.005}$		
$2_1^+ \to 2_5^+$	$-0.048^{+0.002}_{-0.007}$		
$2_1^+ \to 3_1^+$	0.082(5)		
$2_1^+ \to 4_1^+$	0.795(5)	0.71(4)	0.77(4)
$2_1^+ \to 4_2^+$	$-0.22^{+0.05}_{-0.03}$	0.10(2)	
$2_2^+ \to 2_2^+$	$0.26^{+0.02}_{-0.05}$	0.28(6)	
$2_2^+ \to 3_1^+$	$0.52^{+0.02}_{-0.04}$		
$2_2^+ \to 4_2^+$	0.472(6)	0.56(2)	
$4_1^+ \to 4_1^+$	$-0.26^{+0.01}_{-0.07}$	−0.01(5)	
$4_1^+ \to 6_1^+$	$1.11^{+0.03}_{-0.02}$	0.87(2)	
$6_1^+ \to 8_1^+$	$1.25^{+0.07}_{-0.10}$		
$6_1^+ \to 6_1^+$	$-0.23^{+0.09}_{-0.04}$		
$3_1^+ \to 5_1^+$	$0.9^{+0.4}_{-0.6}$		
$4_2^+ \to 3_1^+$	$0.64^{+0.03}_{-0.07}$		
$4_2^+ \to 5_1^+$	$0.9^{+0.7}_{-0.2}$		
$4_2^+ \to 6_2^+$	0.49(3)		
$6_2^+ \to 5_1^+$	$-0.74^{+0.10}_{-0.08}$		
$3_1^+ \to 3_1^+$	$0.13^{+0.08}_{-0.10}$		
$4_2^+ \to 4_2^+$	$-0.24^{+0.08}_{-0.04}$		
$4_1^+ \to 2_2^+$	0.09(2)	−0.11(1)	
$4_1^+ \to 3_1^+$	$-0.44^{+0.08}_{-0.05}$		
$4_1^+ \to 4_2^+$	0.61(1)	−0.10(3)	
$4_1^+ \to 5_1^+$	$-0.08^{+0.09}_{-0.05}$		
$4_1^+ \to 6_2^+$	$-0.186^{+0.030}_{-0.005}$		
$6_1^+ \to 4_2^+$	$0.35^{+0.05}_{-0.03}$	0.21(4)	

Triaxial degrees of freedom

- quadrupole invariants $\langle Q^2 \rangle$ and fluctuations for ground-state and γ bands
- spin independence of invariant shows strong correlations between low-lying states
  $\rightarrow$ rotational behavior
- corresponds to quadrupole deformation $\beta \approx 0.28$

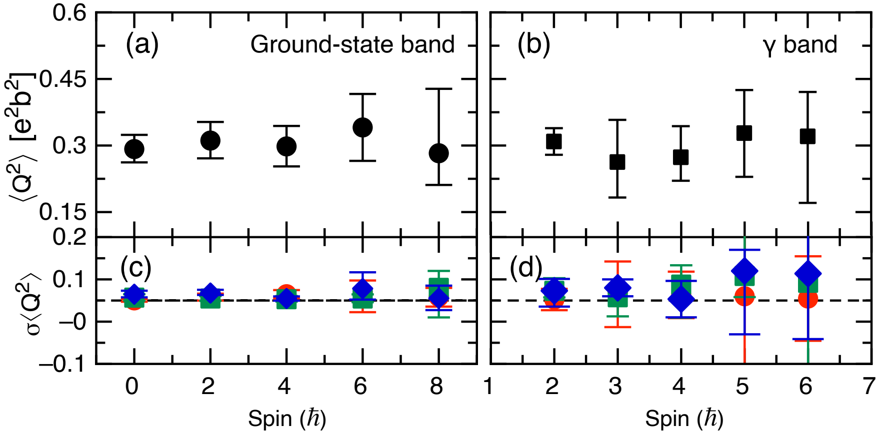

A. D. Ayangeakaa et al., Phys. Rev. Lett. **123** (2019) 102501.

Triaxial degrees of freedom

- $\cos(3\delta) = -1 \rightarrow$ oblate, 0 $\rightarrow$ triaxial ($\delta = \gamma = 30^\circ$), $+1 \rightarrow$ prolate
- almost constant for ground-state and γ band
- average value consistent with triaxial deformation average $\langle\delta\rangle = \approx 27^\circ$ for ground and $\approx 25^\circ$ for γ band

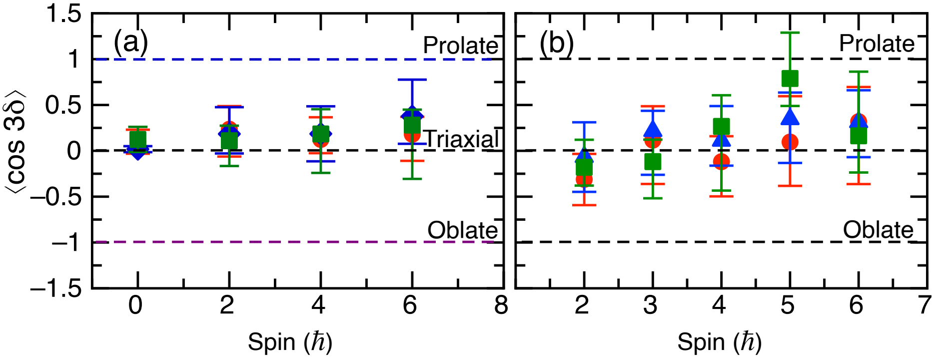

A. D. Ayangeakaa et al., Phys. Rev. Lett. **123** (2019) 102501.

- is it rigid triaxial or γ soft??

Triaxial degrees of freedom

- nature of triaxial deformation can only be inferred from a higher-order invariant, e.g., the statistical fluctuation, or dispersion, $\sigma(\cos(3\delta))$ which determines the degree of rigidity or softness in the γ degree
- ^{76}Ge is one of the very few cases where this analysis has been done

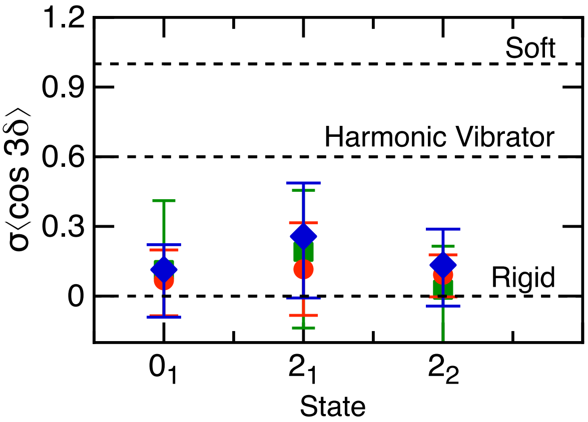

A. D. Ayangeakaa et al., Phys. Rev. Lett. **123** (2019) 102501.

nature of rigid triaxial or γ soft deformation is extremely difficult to asses

Deformation in the $A \sim 100$ region

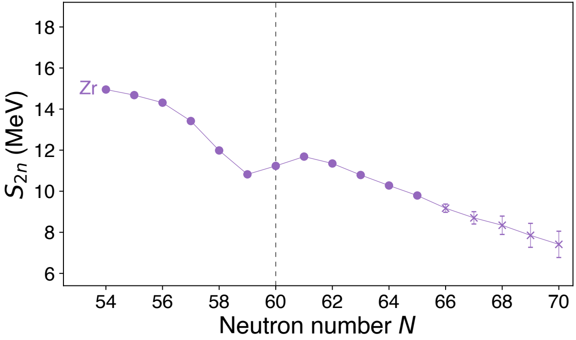

- two-neutrons separation energy S_{2n} drops at sub-shell closures $N = 56, 58$, but rises at $N = 60$ $\rightarrow$ additional binding from deformation
- jump in charge radius at $N = 60$ $\rightarrow$ sudden increase in apparent size arises from deformation
- similar features observed in neighboring isotopic chains
- but not in Kr or Mo $\rightarrow$ island of deformation
- data on isomeric states suggests shape coexistence

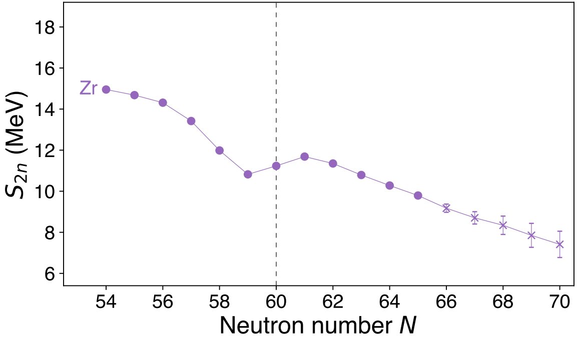

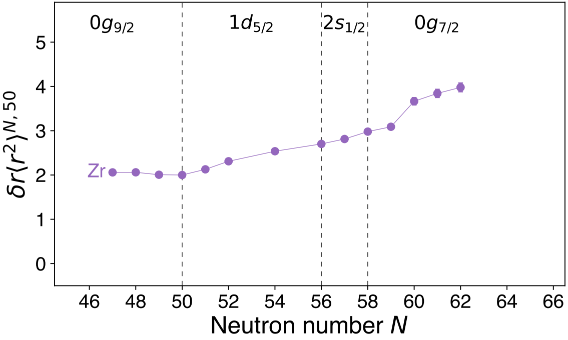

- two-neutrons separation energy S_{2n} drops at sub-shell closures $N = 56, 58$, but rises at $N = 60$ $\rightarrow$ additional binding from deformation
- jump in charge radius at $N = 60$ $\rightarrow$ sudden increase in apparent size arises from deformation
- similar features observed in neighboring isotopic chains
- but not in Kr or Mo $\rightarrow$ island of deformation
- data on isomeric states suggests shape coexistence

Bulk properties, masses and radii

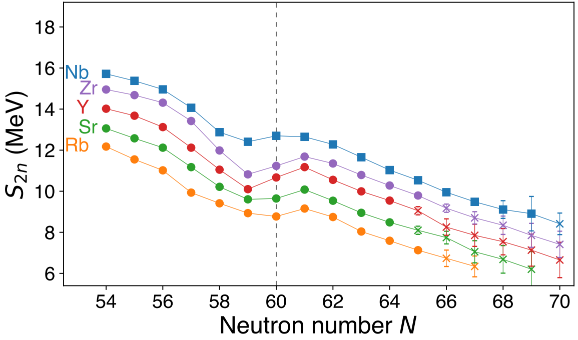

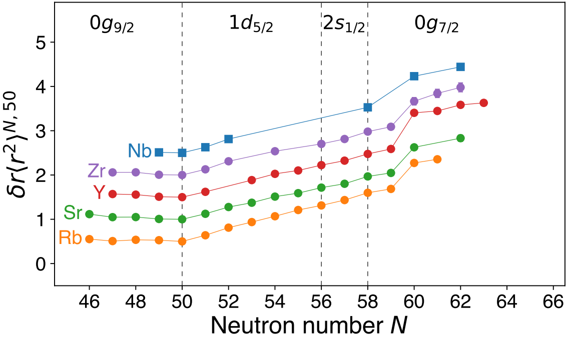

- two-neutrons separation energy S_{2n} drops at sub-shell closures $N = 56, 58$, but rises at $N = 60$ $\rightarrow$ additional binding from deformation
- jump in charge radius at $N = 60$ $\rightarrow$ sudden increase in apparent size arises from deformation
- similar features observed in neighboring isotopic chains
- but not in Kr or Mo $\rightarrow$ island of deformation
- data on isomeric states suggests shape coexistence

Bulk properties, masses and radii

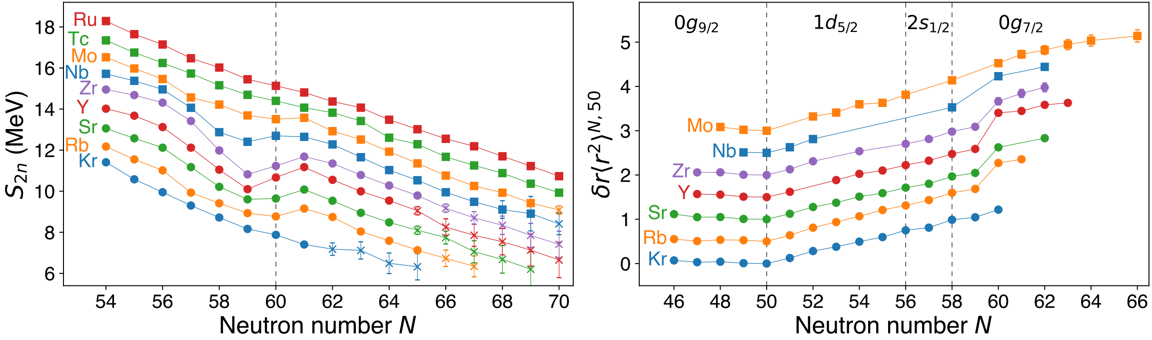

- two-neutrons separation energy S_{2n} drops at sub-shell closures $N = 56, 58$, but rises at $N = 60$ $\rightarrow$ additional binding from deformation
- jump in charge radius at $N = 60$ $\rightarrow$ sudden increase in apparent size arises from deformation
- similar features observed in neighboring isotopic chains
- but not in Kr or Mo $\rightarrow$ island of deformation
- data on isomeric states suggests shape coexistence

Bulk properties, masses and radii

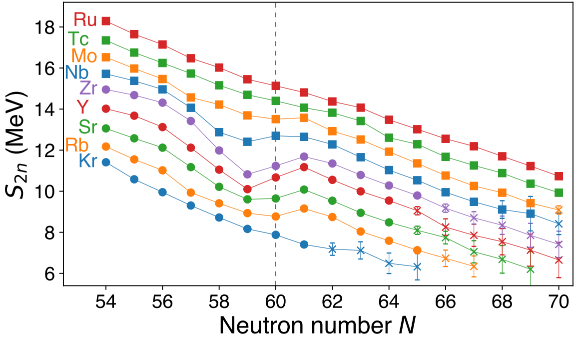

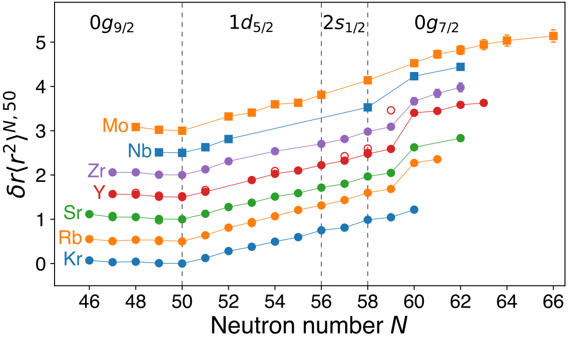

- two-neutrons separation energy S_{2n} drops at sub-shell closures $N = 56, 58$, but rises at $N = 60$ $\rightarrow$ additional binding from deformation
- jump in charge radius at $N = 60$ $\rightarrow$ sudden increase in apparent size arises from deformation
- similar features observed in neighboring isotopic chains
- but not in Kr or Mo $\rightarrow$ island of deformation
- data on isomeric states suggests shape coexistence

Spectroscopy of excited states

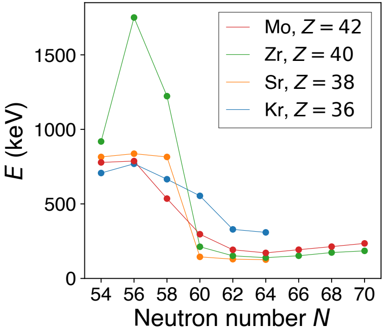

- high energies of ^{96,98}Zr $\rightarrow$ sub-shell closures of the $1d_{5/2}$ and $2s_{1/2}$ orbitals
- sharp drop at $N = 60$ $\rightarrow$ spherical-deformed shape transition
- much smoother decrease for Mo and Kr
- increase in collectivity $B(E2)$ rises from to $\sim$ 100 W.u.
- gradual transition to deformation for Mo and Kr
- $R_{4/2}$ ratio consistent with deformed rotor at and beyond $N = 60$

Spectroscopy of excited states

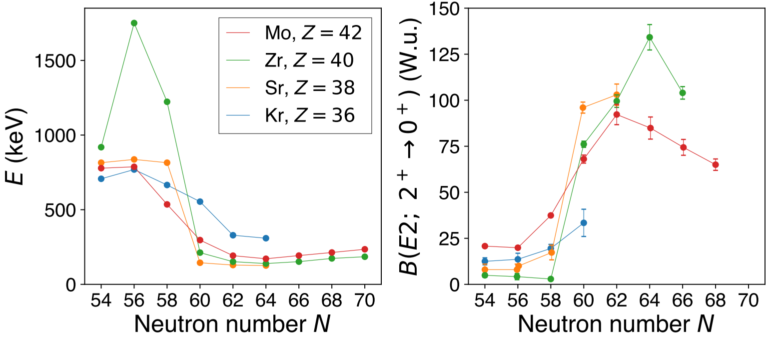

- high energies of ^{96,98}Zr $\rightarrow$ sub-shell closures of the $1d_{5/2}$ and $2s_{1/2}$ orbitals
- sharp drop at $N = 60$ $\rightarrow$ spherical-deformed shape transition
- much smoother decrease for Mo and Kr
- increase in collectivity $B(E2)$ rises from to $\sim$ 100 W.u.
- gradual transition to deformation for Mo and Kr
- $R_{4/2}$ ratio consistent with deformed rotor at and beyond $N = 60$

Spectroscopy of excited states

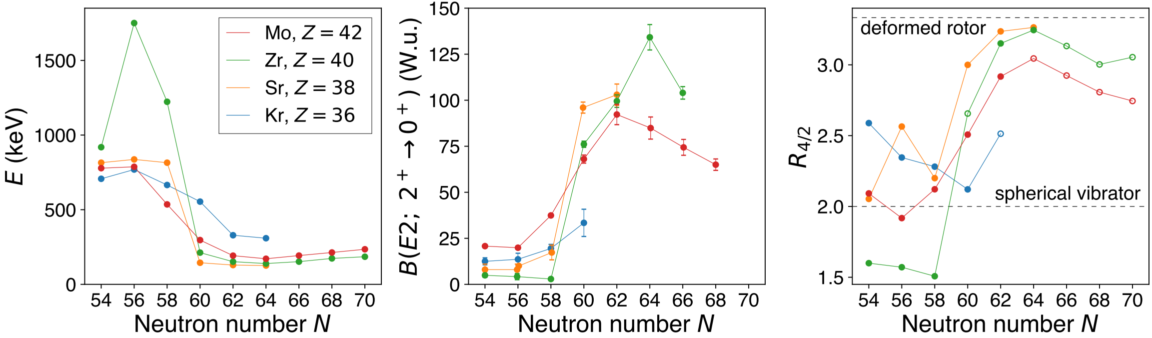

- high energies of ^{96,98}Zr $\rightarrow$ sub-shell closures of the $1d_{5/2}$ and $2s_{1/2}$ orbitals
- sharp drop at $N = 60$ $\rightarrow$ spherical-deformed shape transition
- much smoother decrease for Mo and Kr
- increase in collectivity $B(E2)$ rises from to $\sim$ 100 W.u.
- gradual transition to deformation for Mo and Kr
- $R_{4/2}$ ratio consistent with deformed rotor at and beyond $N = 60$

Shape coexistence

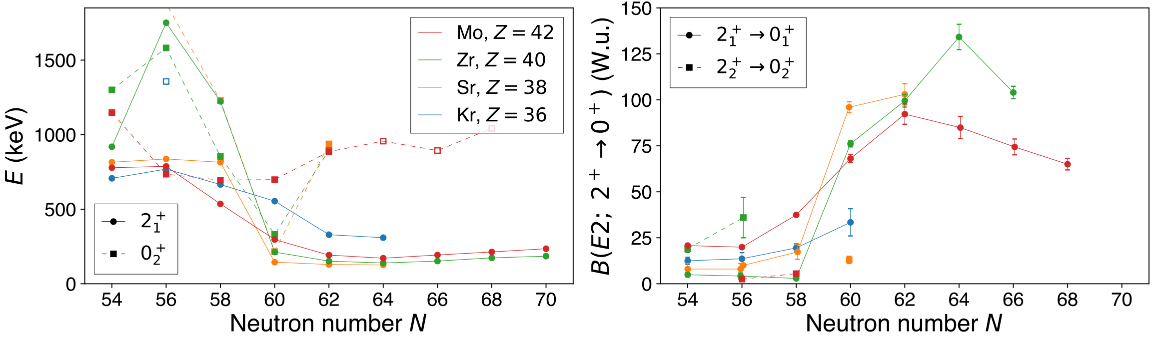

- similar drop of the energy of the excited 0^+ state
- $B(E2;\ 0_2^+ \to 2_2^+)$ very small in ^{98}Sr at $N = 60$
- shape change of the ground state and inversion of configurations
- most rapid onset of deformation in the nuclear chart
- shape coexistence of two or even three configurations of different deformation

Shape coexistence

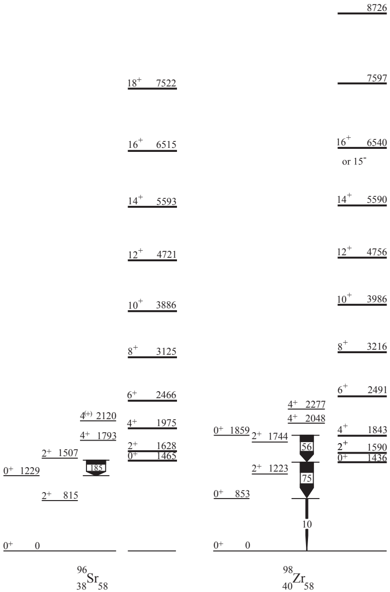

- at $N = 58$ excited strongly deformed band $R_{4/2} \sim 3$
- large electric monopole transitions (large difference in deformation)

K. Heyde, J. L. Wood, Rev. Mod. Phys. **83** (2011) 1467.

Shape coexistence

- at $N = 58$ excited strongly deformed band $R_{4/2} \sim 3$
- large electric monopole transitions (large difference in deformation)

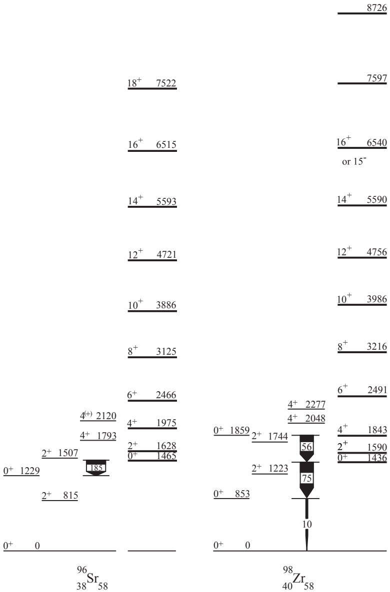

- at $N = 60$, ground state is deformed
- $R_{4/2} = 3.0$ for ^{98}Sr
- large $B(E2)$ values

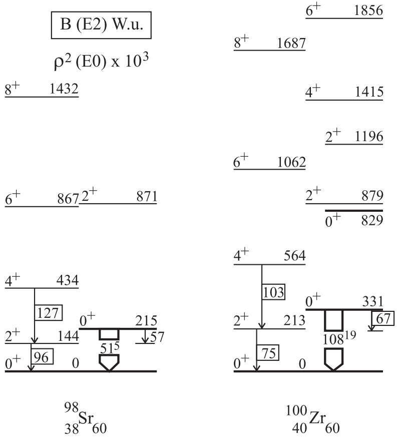

K. Heyde, J. L. Wood, Rev. Mod. Phys. **83** (2011) 1467.

Shape coexistence in Sr nuclei

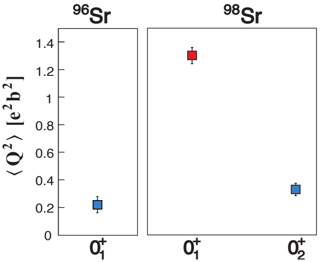

- Coulomb excitation of ^{96,98}Sr: quadrupole moments
  - $\rightarrow$ ^{96}Sr ground state small Q
  - $\rightarrow$ ground state of ^{98}Sr strongly deformed,
  - $\rightarrow$ excited spherical 0^+ state

E. Clément et al., Phys. Rev. Lett. **116** (2016) 022701, Phys. Rev. C **94** (2016) 054326.

- deformed 0^+ state becomes ground state in ^{98}Sr
- large $\rho^2(E0)$ between excited states in ^{96}Sr

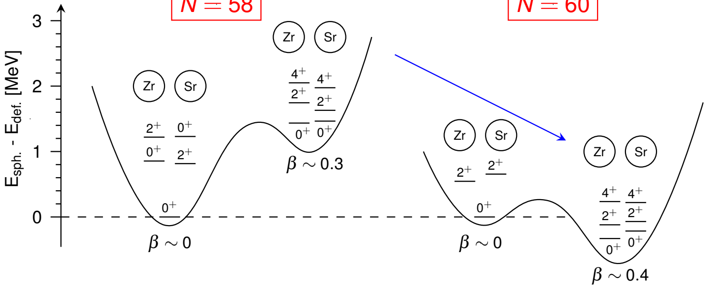

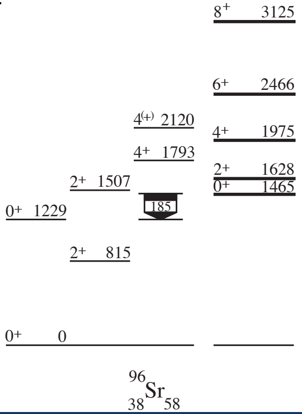

adapted from G. Lhersonneau et al., Phys. Rev. C **49** (1994) 1397.

Federman-Pittel Mechanism

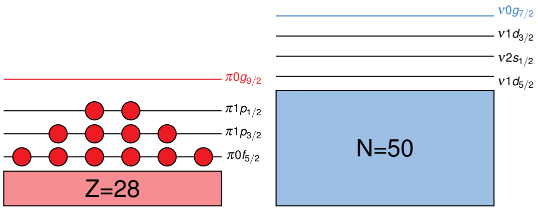

- ^{90}Zr spherical, closed-shell $Z = 40$, $N = 50$
- microscopic, shell model description of deformation

P. Federman and S. Pittel, Phys. Lett. B **69** (1977) 385, Phys. Rev. C **20** (1979) 820.

- excitations to the neutron $0g_{7/2}$ orbital $\rightarrow$ residual $p-n$ interaction lowers proton $0g_{9/2}$ orbital
- increased occupation of the $\pi 0g_{9/2}$ orbital $\rightarrow$ $p-n$ correlations dominate over pairing correlations
- deformed excited configurations at high excitation energy $E_{\text{def}} \gg E_{\text{sph}}$
- ^{100}Zr: drop in excitation energy, deformed ground state

Federman-Pittel Mechanism

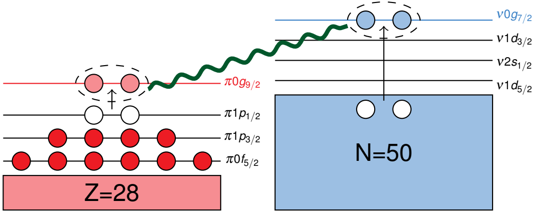

- ^{90}Zr spherical, closed-shell $Z = 40$, $N = 50$
- microscopic, shell model description of deformation

P. Federman and S. Pittel,
Phys. Lett. B **69** (1977) 385, Phys. Rev. C **20** (1979) 820.

- excitations to the neutron $0g_{7/2}$ orbital $\rightarrow$ residual $p - n$ interaction lowers proton $0g_{9/2}$ orbital
- increased occupation of the $\pi 0g_{9/2}$ orbital $\rightarrow$ $p - n$ correlations dominate over pairing correlations
- deformed excited configurations at high excitation energy $E_{\mathrm{def}} \gg E_{\mathrm{sph}}$
- ^{100}Zr: drop in excitation energy, deformed ground state

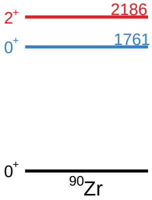

Federman-Pittel Mechanism

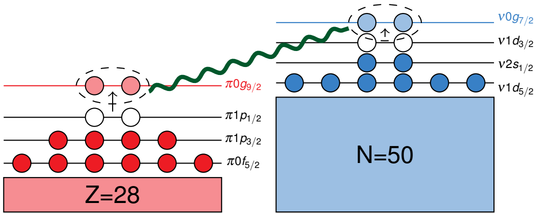

- ^{90}Zr spherical, closed-shell $Z = 40$, $N = 50$
- microscopic, shell model description of deformation

P. Federman and S. Pittel,
Phys. Lett. B **69** (1977) 385, Phys. Rev. C **20** (1979) 820.

- excitations to the neutron $0g_{7/2}$ orbital $\rightarrow$ residual $p - n$ interaction lowers proton $0g_{9/2}$ orbital
- increased occupation of the $\pi 0g_{9/2}$ orbital $\rightarrow$ $p - n$ correlations dominate over pairing correlations
- deformed excited configurations at high excitation energy $E_{\text{def}} \gg E_{\text{sph}}$
- ^{100}Zr: drop in excitation energy, deformed ground state

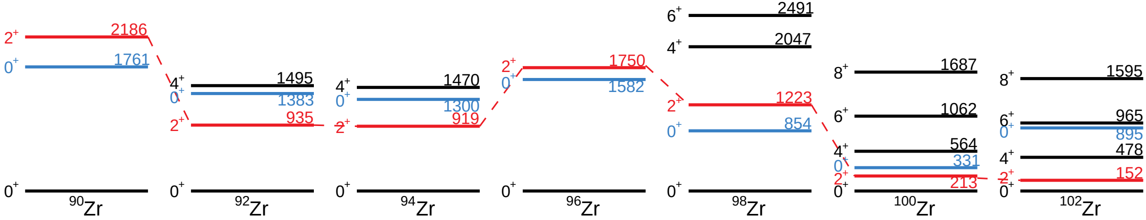

Large-scale shell model calculations

- extended model space:
  $(\pi 1f_{5/2}, 2p_{1/2}, 2p_{3/2}, 1g_{9/2})$
  $(\nu 2d_{5/2}, 3s_{1/2}, 2d_{3/2}, 1g_{7/2}, 1h_{11/2})$
- good description of low-lying states also in even-odd Zr

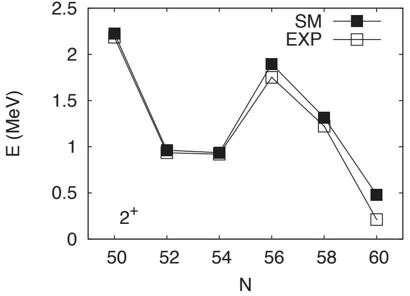

K. Sieja et al., Phys. Rev. C **79** (2009) 064310.

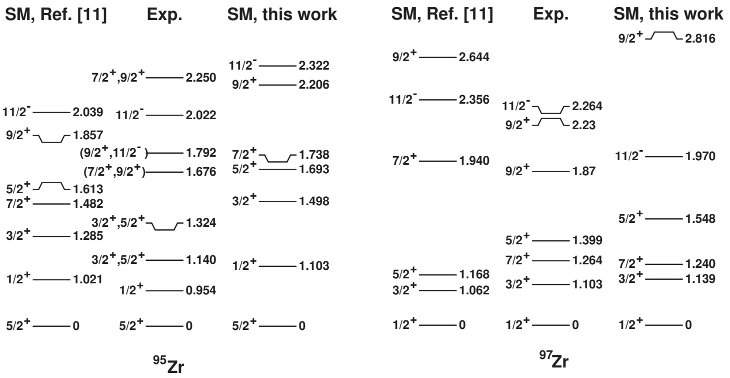

Large-scale shell model calculations

- extended model space:
  $(\pi 1f_{5/2}, 2p_{1/2}, 2p_{3/2}, 1g_{9/2})$
  $(\nu 2d_{5/2}, 3s_{1/2}, 2d_{3/2}, 1g_{7/2}, 1h_{11/2})$
- good description of low-lying states also in even-odd Zr

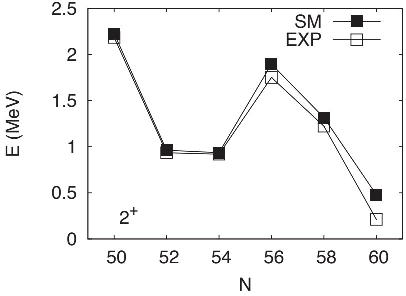

K. Sieja et al., Phys. Rev. C **79** (2009) 064310.

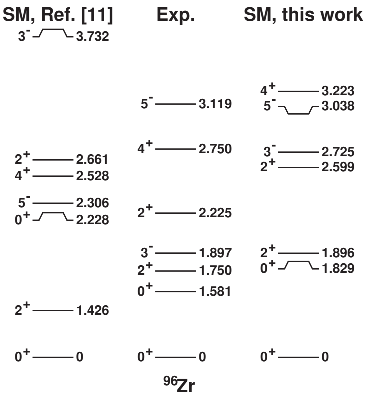

	$0f_{5/2}$	$1p_{3/2}$	$1p_{1/2}$	$0g_{9/2}$	$1d_{5/2}$	$2s_{1/2}$	$0g_{7/2}$	$1d_{3/2}$	$0h_{11/2}$
0_1^+	5.64	3.68	1.76	0.90	5.26	0.12	0.17	0.16	0.27
0_2^+	5.43	3.31	1.13	2.11	4.10	0.63	0.45	0.49	0.32

- mixed configuration of excited configuration
- octupole 3^- state underestimated

Monte-Carlo shell model calculations

- microscopic description of shapes change as a function of proton or neutron number
- proton-neutron interaction changes the ordering and spacing of levels
- (near-) degeneracy triggers symmetry breaking and deformation
- calculations reproduce the abrupt shape change in Zr

T. Togashi et al., Phys. Rev. Lett. **117** (2016) 172502.

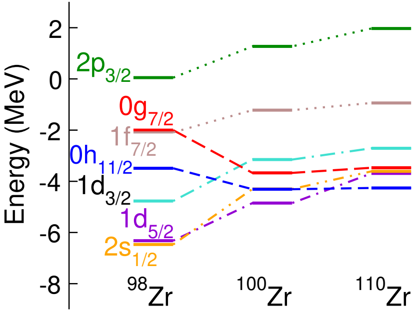

Monte-Carlo shell model calculations

- microscopic description of shapes change as a function of proton or neutron number
- proton-neutron interaction changes the ordering and spacing of levels
- (near-) degeneracy triggers symmetry breaking and deformation
- calculations reproduce the abrupt shape change in Zr

T. Togashi et al., Phys. Rev. Lett. **117** (2016) 172502.

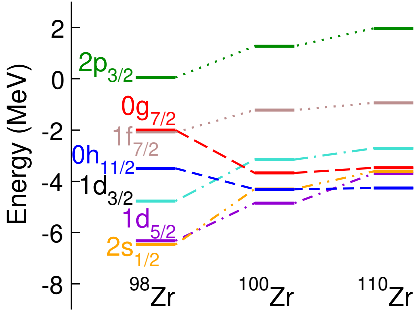

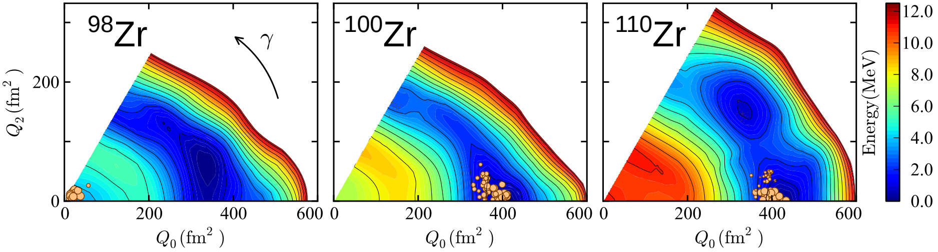

Summary

- deformation is not observable, but affects many observables
- β can be inferred from measurements of excitation energies, quadrupole moments, and transition rates
- always model dependent
- quadrupole rotationally invariant sum rules provide a more model independent measure of the shape
  $\rightarrow$ but are very hard to obtain experimentally
- how does shape coexistence matter?
- question of the nature of triaxial deformation, rigid or soft

Thank you for your attention

The case of ^{96}Ru and ^{96}Zr

Properties of ^{96}Zr

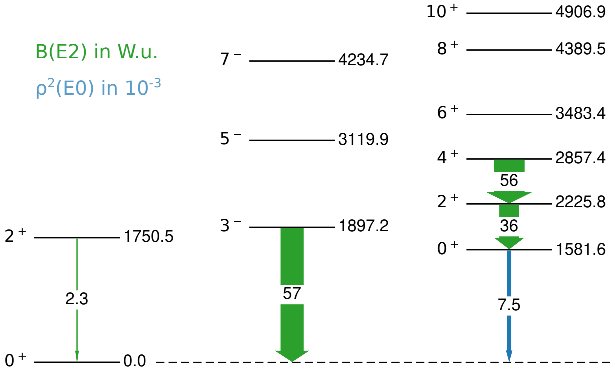

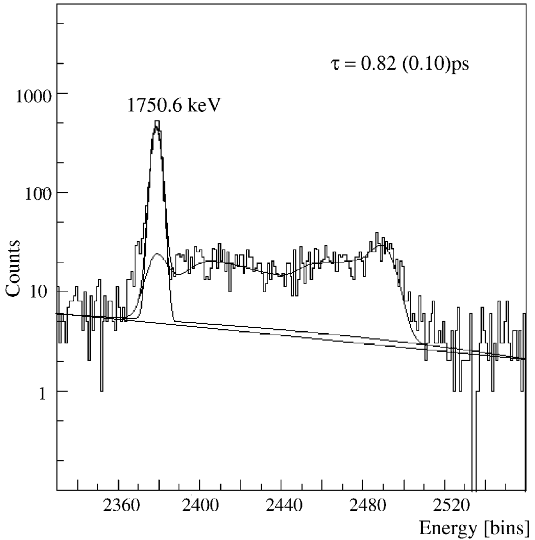

- proton and neutron removal transfer reactions: ground state configuration $\pi(1p_{1/2})^2\nu(1d_{5/2})^6$
- closed shell configuration with $N = 56$ and $Z = 40$
- high 2_1^+ state, with small $\beta = 0.062(3)$ from $B(E2;\, 0_1^+ \rightarrow 2_1^+) = 2.3(3)$ W.u.

G. Kumbartzki et al., Phys. Lett. B **562** (2003) 193.

Properties of ^{96}Zr

- only one measurement for $B(E2;\,0_1^+ \to 2_1^+)$ but compilations also cite a publication for 1965 "Coulomb Excitation of the First 2^+ Levels of ^{90}Zr and ^{96}Zr" with an almost two times larger $B(E2)$

S. Raman et al., At. Data Nucl. Data Tables **78** (2001) 1, Y. P. Gangrskii, I. K. Lemberg, Yadern. Fiz. **1** (1965) 1025.

- quadrupole moment and branch ratio to 0_2^+ unknown

- 2_2^+ state populated using electron scattering
- $B(E2;\,0_1^+ \to 2_2^+)$ can be extracted relative to the $B(E2;\,0_1^+ \to 2_1^+)$ value
- known decay branching ratios of 2_2^+ allow to extract $B(E2;\,2_2^+ \to 0_2^+) = 36(11)$ W.u.
- collective, similar deformation for 2_2^+ and 0_2^+, assuming rigid axial rotor $\beta = 0.24$
- two decoupled configurations with different deformation
- supported by calculations and two-state mixing model
- shape coexistence

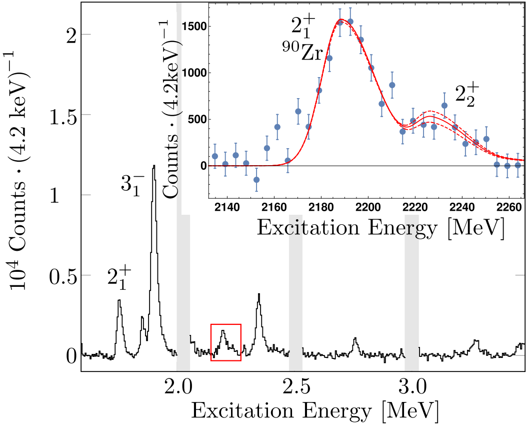

C. Kremer et al., Phys. Rev. Lett. **117** (2016) 172503.

Properties of ^{96}Zr

- only one measurement for $B(E2;\ 0_1^+ \rightarrow 2_1^+)$ but compilations also cite a publication for 1965 “Coulomb Excitation of the First 2^+ Levels of ^{90}Zr and ^{96}Zr” with an almost two times larger $B(E2)$

S. Raman et al., At. Data Nucl. Data Tables **78** (2001) 1, Y. P. Gangrskii, I. K. Lemberg, Yadern. Fiz. **1** (1965) 1025.

- quadrupole moment and branch ratio to 0_2^+ unknown

- 2_2^+ state populated using electron scattering
- $B(E2;\ 0_1^+ \rightarrow 2_2^+)$ can be extracted relative to the $B(E2;\ 0_1^+ \rightarrow 2_1^+)$ value
- known decay branching ratios of 2_2^+ allow to extract $B(E2;\ 2_2^+ \rightarrow 0_2^+) = 36(11)$ W.u.
- collective, similar deformation for 2_2^+ and 0_2^+, assuming rigid axial rotor $\beta = 0.24$
- two decoupled configurations with different deformation
- supported by calculations and two-state mixing model
- shape coexistence

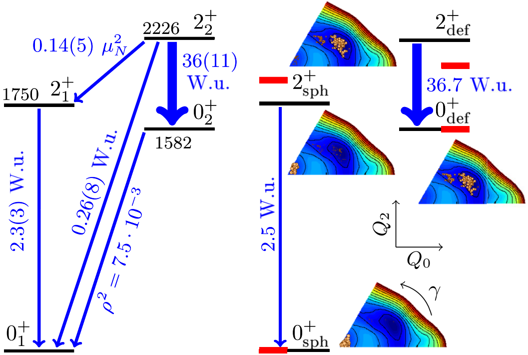

C. Kremer et al., Phys. Rev. Lett. **117** (2016) 172503.

Octupole deformation of ^{96}Zr

- octupole correlations are dominant in regions where $\Delta l = \Delta j = 3$ orbitals are close to the Fermi surface
- proton $1p_{3/2} - 0g_{9/2}$ and $1d_{5/2} - 0h_{11/2}$ excitations across $Z = 40$ and $N = 56$
- large $B(E3;\, 3^-_1 \rightarrow 0^+_1)$ values from lifetime measurements and proton inelastic scattering

- direct lifetime measurement following ^{96}Y β decay yields 65(10) W.u.

  H. Mach et al., Phys. Rev. C **42** (1990) 811.
- Doppler-shift lifetime measurement: $B(E3) = (47.1 \pm 4.7)$ W. u.

  D. J. Horen et al., Phys. Rev. C **48** (1993) R2131.
- large uncertainties, yet the most enhanced one-phonon $0^+_1 \rightarrow 3^-_1$ transition observed
- axial symmetry

$$\beta_3 = \frac{4\pi}{3eZR^3}\sqrt{B(E2;\, 0^+_1 \rightarrow 3^-_1)}$$

yields $\beta_3 \sim 0.25$

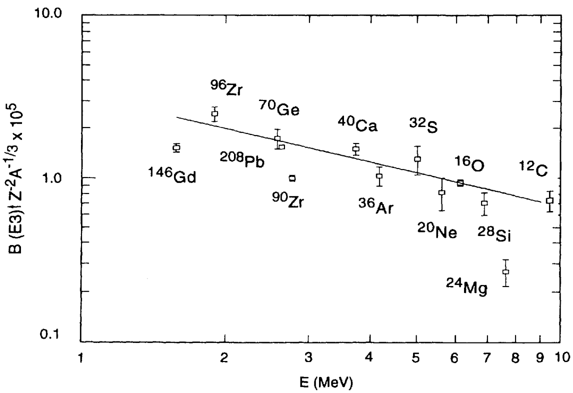

Structure of ^{96}Ru

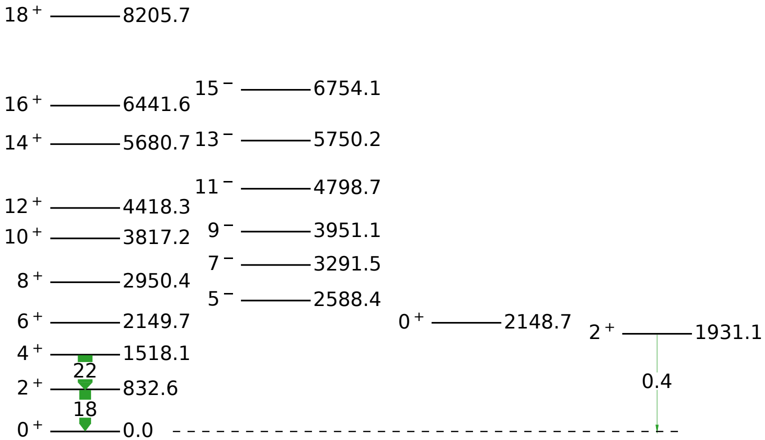

H. Klein et al., Phys. Rev. C **65** (2002) 044315.

- $B(E2;\ 0_1^+ \rightarrow 2_1^+) = 18.2$ W.u.
- c.f. 2.3 W.u. for ^{96}Zr
- $\beta_2 = 0.154$
- moderately deformed ground state band
- $Q = -0.13(9)$ prolate, but with very large uncertainty

S. Landsberger et al., Phys. Rev. C **21** (1980) 588.

- excited 0^+ state known
- many lifetimes known
- transfer reactions (p, d) shows distribution of strength over several levels
  $\rightarrow$ consistent with deformation

Summary

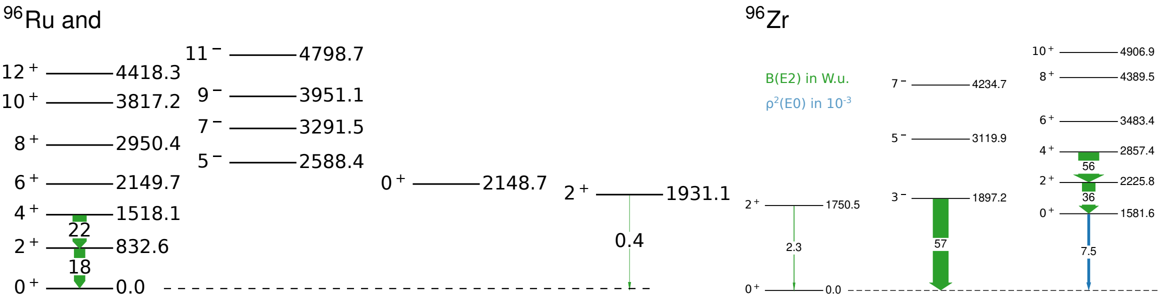

- are two very different nuclei

Thank you for your attention